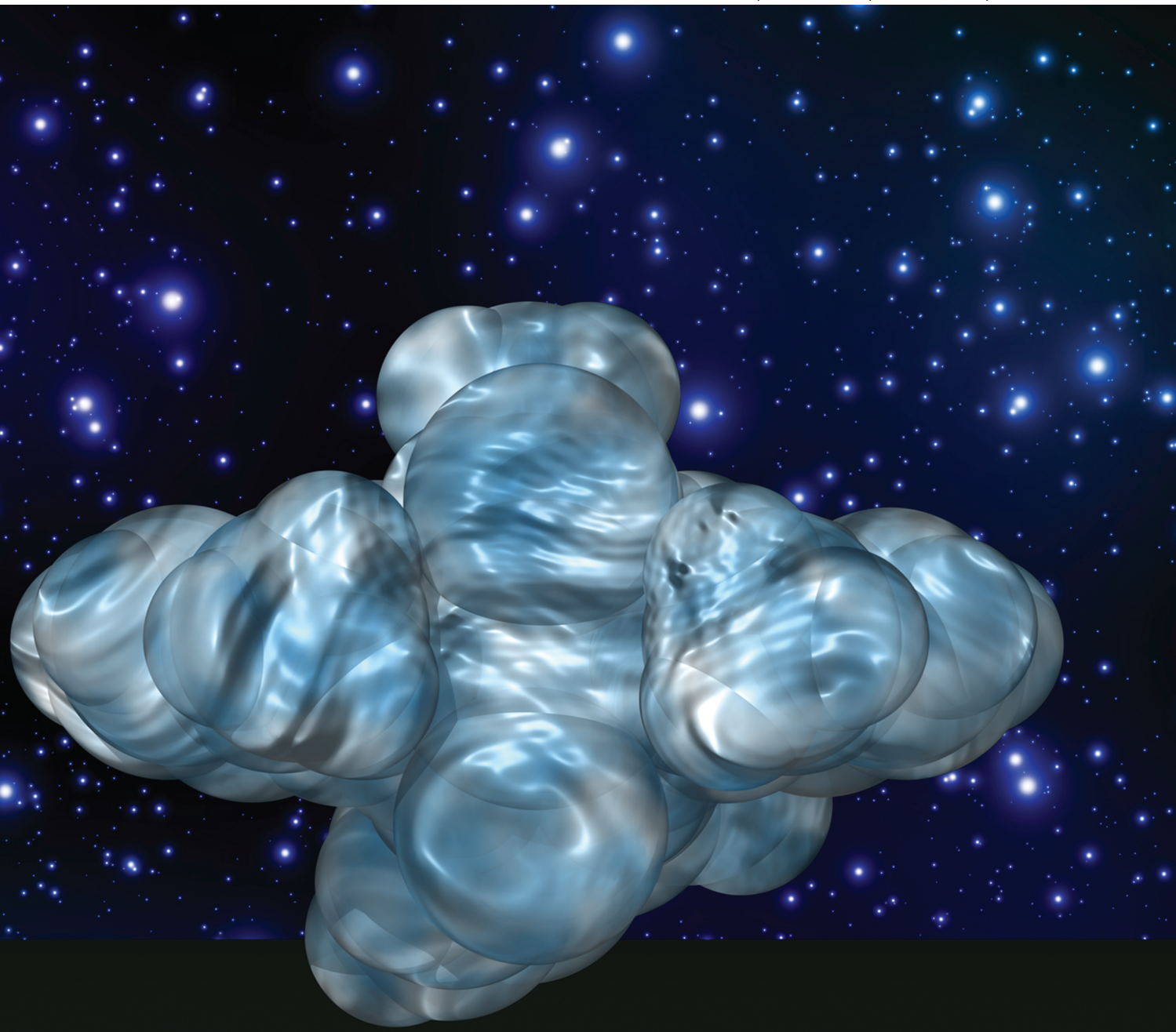


Dalton Transactions

An international journal of inorganic chemistry

www.rsc.org/dalton

Volume 41 | Number 13 | 7 April 2012 | Pages 3585–3844



ISSN 1477-9226

RSC Publishing

COVER ARTICLE

Halcrow *et al.*

Iron(II) complexes of new hexadentate 1,1,1-tris(iminomethyl)ethane podands, and their 7-methyl-1,3,5-triazaadamantane rearrangement products

Iron(II) complexes of new hexadentate 1,1,1-tris-(iminomethyl)ethane podands, and their 7-methyl-1,3,5-triazaadamantane rearrangement products†

Sara A. Diener,^{a,b} Amedeo Santoro,^a Colin A. Kilner,^a Jonathan J. Loughrey^a and Malcolm A. Halcrow^{*a}

Received 11th October 2011, Accepted 5th December 2011

DOI: 10.1039/c2dt11911k

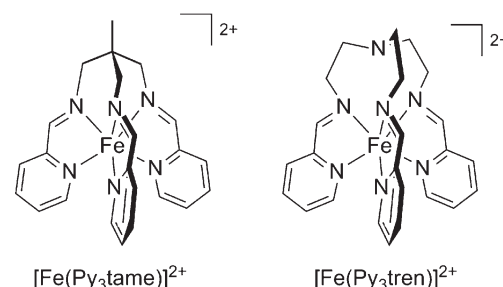
New iron(II) podand complexes have been prepared, by condensation of 2-(aminomethyl)-2-methyl-1,3-diaminopropane with 3 equiv of a heterocyclic aldehyde in the presence of hydrated $\text{Fe}[\text{BF}_4]_2$ or $\text{Fe}[\text{ClO}_4]_2$ as templates. The 2-(aminomethyl)-2-methyl-1,3-diaminopropane is prepared *in situ* by deprotonation of its trihydrochloride salt. The chloride must be removed from these reactions by precipitation with silver, to avoid the formation of the alternative 2,4,6-trisubstituted-7-methyl-1,3,5-triazaadamantane condensation products, or their FeCl_2 adducts. The crystal structures of two 2,4,6-tri(pyridyl)-7-methyl-1,3,5-triazaadamantane-containing species are presented, and contain two different geometric isomers of this tricyclic ring with three equatorial, or two equatorial and one axial, pyridyl substituents. Both structures feature strong C–H…X ($X = \text{Cl}$ or F) hydrogen bonding from the aminal C–H groups in the triazaadamantane ring. Five iron(II) podand complexes were successfully obtained, all of which contain low-spin iron centres.

Introduction

Although the phenomenon was first identified 40 years ago,¹ the continued interest in the synthesis of new spin-transition compounds^{2,3} stems from their potential applications as switchable materials in display and memory devices,⁴ in medical imaging,⁵ in switchable polymers^{6,7} or liquid crystals,^{7,8} and in nanotechnology.^{7,9} Most application studies of spin-transition compounds have been carried out using only two classes of material: iron(II)–triazole 1-D coordination polymers,¹⁰ or Hoffman network compounds $[\text{Fe}(\text{L})\text{M}(\text{CN})_6]$ (L = pyrazine or 4,4'-azopyridine; $\text{M} = \text{Ni}$, Pd or Pt).¹¹ Hence, there is still a need for new spin-crossover materials that show technologically favourable switching properties,¹² which is driving the continued search for new examples.

The complex $[\text{Fe}(\text{Py}_3\textrm{tame})]^{2+}$ ($[\text{Fe}(\mathbf{1A})]^{2+}$, see below) was studied extensively in the early 1970s, with regard to its ligand-imposed distorted six-coordinate geometry.^{13–15} It is low-spin at room temperature and below in the solid state,¹⁴ and at temperatures up to 368 K in solution.¹⁵ However, it has recently been reported that some liquid crystalline $[\text{Fe}(\text{Py}_3\textrm{tame})]^{2+}$ analogues bearing 5-alkoxy-6-methylpyridyl donors undergo very gradual

thermal spin-transitions above room temperature.¹⁶ This is reminiscent of the well-known series of complexes based on the $\text{Py}_3\textrm{tren}$ podand. Although $[\text{Fe}(\text{Py}_3\textrm{tren})]^{2+}$ itself is also low-spin, it can be converted to a spin-crossover centre by introducing 6-methyl substituents onto its pyridyl rings,¹⁷ or by replacing them with other heterocyclic donors such as imidazol-2-yl,¹⁸ imidazol-4-yl^{19–21} or pyrazol-3-yl groups.^{22,23} With this in mind, as a continuation of our own interest in spin-crossover compounds²⁴ we have investigated analogues of $[\text{Fe}(\text{Py}_3\textrm{tame})]^{2+}$ bearing different heterocyclic substituents. In addition to these products, this work has afforded the first crystallographic characterisation of 2,4,6-trisubstituted-1,3,5-triazaadamantane derivatives, which are rearrangement products of the $\text{Py}_3\textrm{tame}$ ligand.¹³ Another study containing two $[\text{Fe}(\text{Py}_3\textrm{tame})]^{2+}$ analogues has also been recently published, by Gütlich *et al.*²⁵



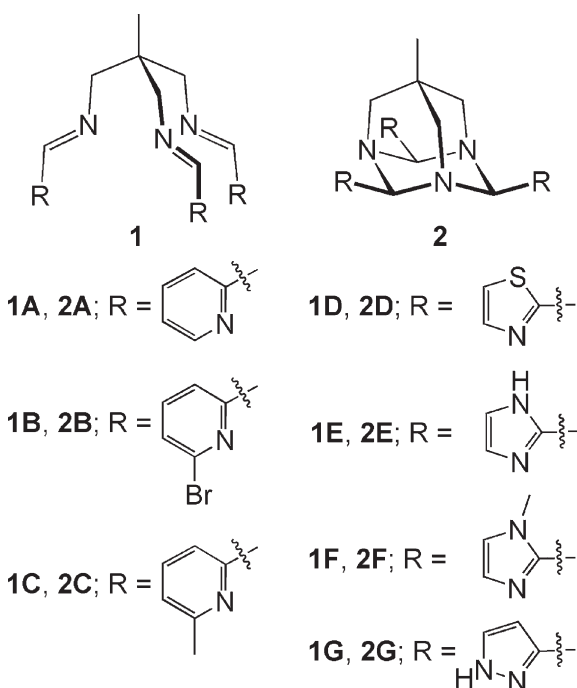
^aSchool of Chemistry, University of Leeds, Woodhouse Lane, Leeds, U.K., LS2 9JT. E-mail: M.A.Halcrow@leeds.ac.uk; Fax: (+44) 113 343 6565; Tel: (+44) 113 343 6506

^bDepartment of Chemistry, Mail #OSS402, University of St. Thomas, 2115 Summit Avenue, St. Paul, MN 55105-1096, USA

† Electronic supplementary information (ESI) available: additional crystallographic figures and tables for the compounds in this work. CCDC reference numbers 848507–848511. For ESI and crystallographic data in CIF or other electronic format see DOI: 10.1039/c2dt11911k

Results and discussion

Complexes of the $[\text{Fe}(\text{Py}_3\textrm{tame})]^{2+}$ type ($[\text{Fe}L]^{2+}$, $L = \mathbf{1A–1G}$; Scheme 1) must be prepared by a metal-templated condensation



Scheme 1 Organic compounds referred to in this work. **1A** is Py₃tame.

of 2-(aminomethyl)-2-methyl-1,3-diaminopropane with 3 equiv of the appropriate aldehyde. In the absence of the templating ion, the 2,4,6-trisubstituted-7-methyl-1,3,5-triazaadamantane *tris*-aminals (**2A–2G**; Scheme 1) are formed preferentially, which can only be induced to ring-open under prolonged aqueous reflux.¹³ The precursor amine 2,2-*bis*(aminomethyl)-1-aminopropane is commercially available as its *tris*-hydrochloride salt, which was neutralised with NaOH *in situ* prior to the reaction. Initial attempts to perform such reactions in ethanol, using hydrated Fe[BF₄]₂ as template, led to the adducts [FeCl₂(**2**)] rather than the desired products [Fe(**1**)][BF₄]₂. This led us to conclude that the chloride in the reaction mixture was interfering with the template condensation reaction. The triazaadamantane complexes are recognisable by their sparing solubility and yellow colouration. The full characterisation and crystal structure of one such product, [FeCl₂(**2C**)], is described below.

The formation of triazaadamantane adducts under the above reaction conditions is avoided by removal of the chloride by precipitation with AgBF₄, before addition of the iron salt and aldehyde reagents. This procedure successfully afforded the podand complexes [FeL][BF₄]₂ (*L* = **1C**, **1D** and **1F**) in moderate yields. Alternatively, performing the syntheses in water rather than ethanol removes the requirement for chloride precipitation, although the yields of [Fe(**1**)][BF₄]₂ were lower by this route. Moreover, some of the BF₄[−] salts were hygroscopic or retained organic solvents, which made them difficult to obtain in pure form. These issues were overcome by using perchlorate as counterion, which gave higher yields of more tractable crystalline products from the aqueous syntheses. Thus, [FeL][ClO₄]₂ (*L* = **1C**, **1E** and **1G**) were obtained as pure anhydrous, or hydrated, solids ([Fe(**1C**)][ClO₄]₂ has been reported previously²⁵).

Finally, when 6-bromo-pyridine-2-carbaldehyde was used as the reagent under any of these conditions, the protonated

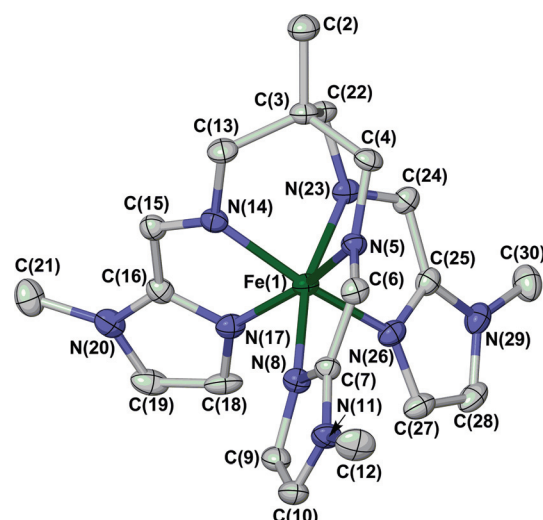


Fig. 1 View of the complex dication in the crystal structure of [Fe(**IF**)][BF₄]₂. All H atoms have been omitted for clarity, and displacement ellipsoids are at the 50% probability level.

adamantane [**2BH**]BF₄ was the only isolable product. It may be that the bromo substituents *ortho* to the putative pyridyl ligand donor groups are too bulky to support the [Fe(**1B**)]²⁺ podand structure.

All of the [Fe*L*]²⁺ (*L* = **1C–1G**) complexes are intensely coloured and are low-spin at room temperature, from their solid state magnetic moments ($\chi_{MT} \leq 0.2 \text{ cm}^3 \text{ mol}^{-1} \text{ K}$) and by ¹H NMR in solution. The ¹H NMR spectra in CD₃NO₂ show a single *C*₃-symmetric ligand environment, as expected, although all the compounds except for [Fe(**ID**)][BF₄]₂ show significant peak broadening. This broadening probably reflects inversion of the helical conformation adopted by the coordinated ligands, on the NMR timescale.¹⁵ The only compounds to show some evidence of isotropic shifting are [Fe(**IC**)][ClO₄]₂ and [Fe(**IG**)][ClO₄]₂, whose N=CH imine resonances occur at 12–15 ppm, up to 6 ppm higher than for the other podand complexes. This implies a small fraction of those compounds is paramagnetic and high-spin under these conditions,²⁷ and thus that they may undergo spin-crossover in solution centred significantly above room temperature (a fully high-spin complex of this type should exhibit this ¹H peak near 250 ppm).²² This small stabilisation of the high-spin state is probably a consequence of steric crowding of the methyl substituents in [Fe(**IC**)]²⁺¹⁷ and the weaker basicity of the pyrazole donors in [Fe(**IG**)]²⁺.²²

Single crystal X-ray structures were obtained of [Fe(**IF**)][BF₄]₂ (Fig. 1), [Fe(**IG**)][ClO₄]₂ (Fig. 2) and hydrated crystals of [Fe(**IE**)][ClO₄]₂, which showed Fe–N bond lengths of 1.95–2.02, as expected for low-spin iron(II) centres (ESI†).²⁶ The crystal structure of [Fe(**IE**)][ClO₄]₂·0.7H₂O deserves further comment. Its asymmetric unit contains two formula units, one of which is completely disordered over two sites in a 0.6 : 0.4 occupancy ratio (Fig. 3). This disorder is not caused by the iron centres adopting a mixed high–low spin-state population,²⁸ since the Fe–N bond lengths in the major and minor disorder sites are equal within experimental error (ESI†). Rather, it reflects the presence of an additional 40%-occupied water molecule in the minor disorder site [O(76B), Fig. 3]. This water molecule

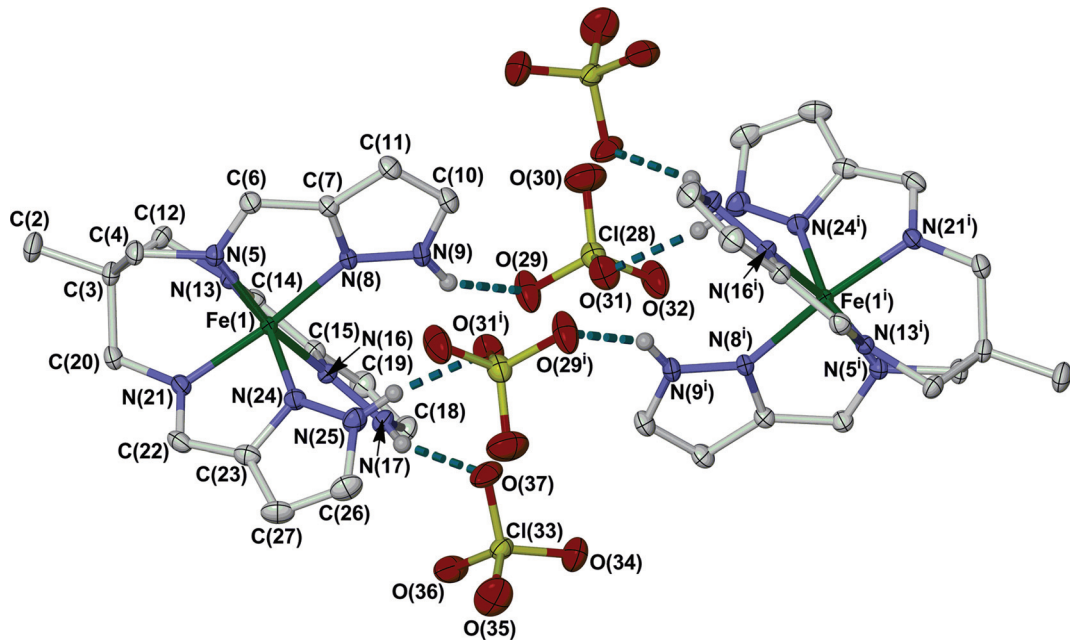


Fig. 2 View of $[\text{Fe}(\text{IG})][\text{ClO}_4]_2$, showing the association of the salt into a centrosymmetric hydrogen bonded dimer. All C-bound H atoms have been omitted for clarity, and displacement ellipsoids are at the 50% probability level. Symmetry code: (i) $-x, -y, -z$. Colour code: C, white; H, grey; Cl, yellow; Fe, green; N, blue; O, red.

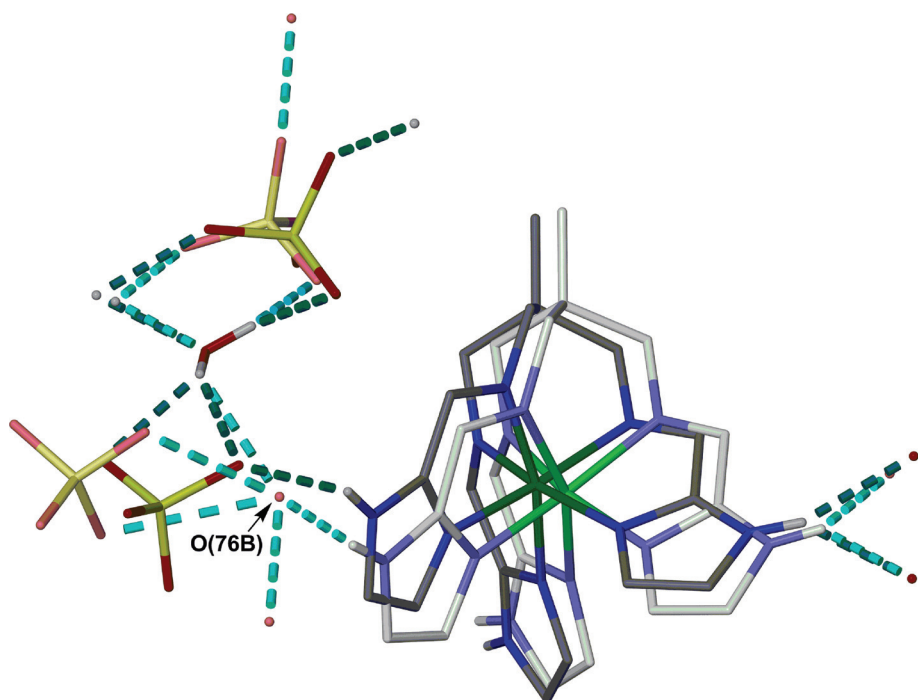


Fig. 3 View showing the disordered region of the asymmetric unit in $[\text{Fe}(\text{IE})][\text{ClO}_4]_2 \cdot 0.7\text{H}_2\text{O}$. C-bound H atoms have been omitted, and all atoms have arbitrary radii. The atoms and hydrogen bonds in the major and minor disorder sites are shown in dark and pale colouration, respectively, and the partial water molecule that causes the disorder is labelled for clarity. The crystallographically ordered water site is included, but hydrogen bonds to other ordered residues are not shown. Views of the full asymmetric unit are given in the ESI†. Other details as in Fig. 2.

displaces the neighbouring complex cation by *ca.* 0.5 Å, and the nearest neighbour anion by 1.7 Å, from their positions when this site is unoccupied. If the ‘A’ disorder isomer is considered in isolation, the disordered cation is four-connected and the

crystallographically ordered water molecule is five-connected, while the ordered cation is only two-connected and so is ignored in the topological analysis (ESI†). The resultant hydrogen bonded network forms 2D sheets parallel to (100) with $3^24^3.34^3$

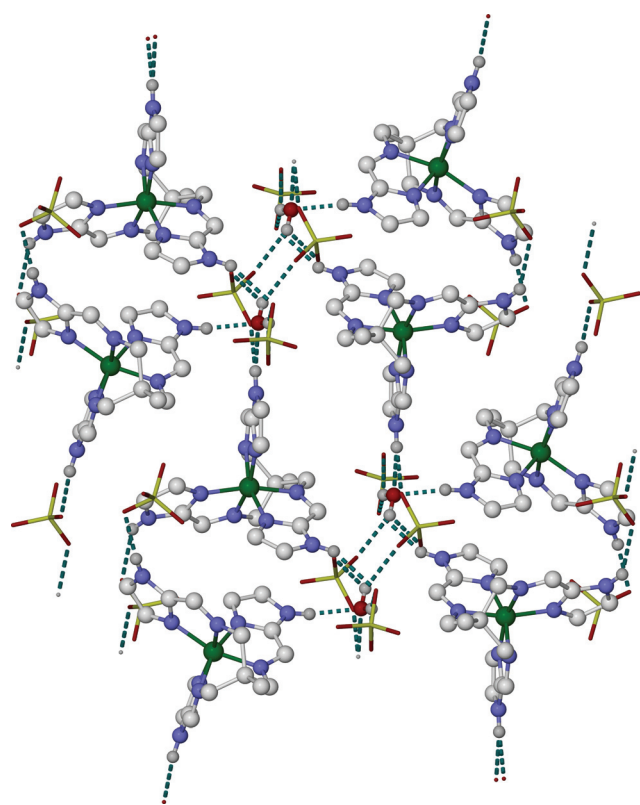


Fig. 4 Packing diagram of the ‘A’ disorder structure of $[\text{Fe}(\text{IE})_2][\text{ClO}_4]_2 \cdot 0.7\text{H}_2\text{O}$, showing the association of the compound into hydrogen-bonded sheets. All atoms have arbitrary radii, C-bound H atoms are omitted, and the ClO_4^- ions are de-emphasised for clarity. The view is perpendicular to the $[100]$ vector. Other details as in Fig. 2.

connectivity in the short Schäfli notation (Fig. 4). In the ‘B’ disorder structure, the disordered cation and ordered water are now both five-connected in their hydrogen bonding, while the ordered cation is two-connected as before. The extra water node O(76B) is four-connected (Fig. 3), and extends the network into the third dimension.

The complex cations in $[\text{Fe}(\text{IG})][\text{ClO}_4]_2$ associate into centrosymmetric dimers, *via* N–H···O interactions to bridging perchlorate anions (Fig. 2). There are no noteworthy intermolecular contacts in $[\text{Fe}(\text{IF})][\text{BF}_4]_2$ (ESI†).

The asymmetric unit of $[\text{FeCl}_2(\text{2C})]\cdot n\text{H}_2\text{O}$ ($n \approx 1$) also contains two formula units. The two unique iron centres have almost identical five-coordinate structures (Fig. 5 and 6), with the **2C** ligands binding in tridentate fashion through one tertiary amino donor and two of the three pendant pyridyl groups. The iron centres are high-spin, as expected for a complex with this ligand set, which is consistent with the compound’s room-temperature magnetic moment ($\chi_M T = 3.4 \text{ cm}^3 \text{ mol}^{-1} \text{ K}$).²⁹ The coordination geometry is best described as distorted square pyramidal ($\tau = 0.33$ and 0.36)³⁰ but with no obvious apical ligand site; the two Fe–Cl bond lengths in each molecule are almost equivalent (ESI†). This intermediate coordination geometry may be imposed by the methyl substituents on the two pyridyl donor groups, which are in van der Waals contact with the two chloride ligands. The two unique complex molecules associate into a head-to-tail dimer through weak C–H···Cl interactions from

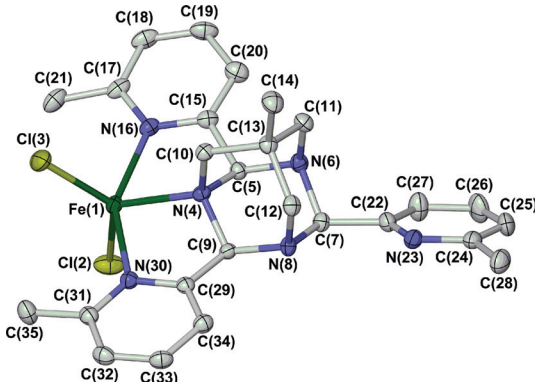


Fig. 5 View of one of the two unique molecules in the crystal structure of $[\text{FeCl}_2(\text{2C})]\cdot n\text{H}_2\text{O}$. All H atoms have been omitted for clarity, and displacement ellipsoids are at the 50% probability level. Other details as in Fig. 2.

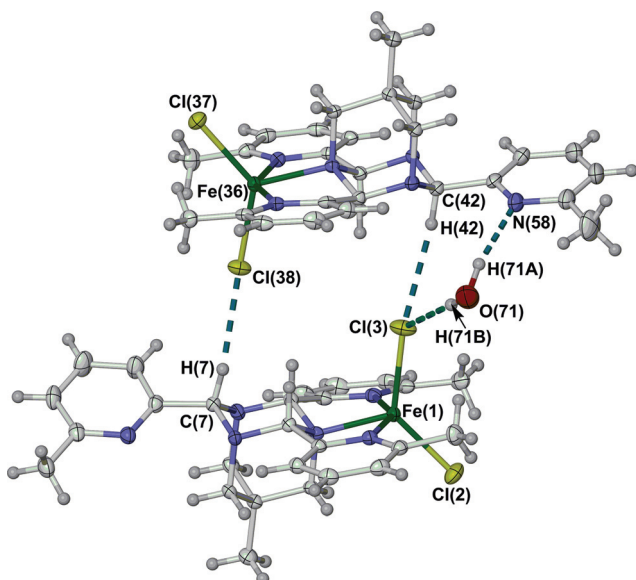


Fig. 6 View of the dimeric moiety in the crystal structure of $[\text{FeCl}_2(\text{2C})]\cdot n\text{H}_2\text{O}$. Only atoms involved in hydrogen bonding interactions are labelled. Displacement ellipsoids are at the 50% probability level apart from hydrogen atoms, which have arbitrary radii. Other details as in Fig. 2.

relatively acidic aminal C–H groups ($\text{H}\cdots\text{Cl} = 2.8\text{--}2.9 \text{ \AA}$, $0.1\text{--}0.2 \text{ \AA}$ shorter than the sum of their van der Waals radii,³¹ Fig. 6). A water molecule also links the molecules on one side of the dimer, by hydrogen bonding to a chloride ligand from one molecule and the pendant pyridyl group of the other (Fig. 6). Adjacent dimers in the lattice related by the crystallographic C_2 axis interdigitate *via* inter-dimer $\pi\cdots\pi$ interactions between coordinated pyridyl groups, to form sheets of molecules along the (001) crystal plane (ESI†). The remaining water content in the crystal is disordered within channels of approximate dimensions $4.2 \times 3.8 \text{ \AA}$, running parallel to the unit cell a axis.

Finally, the triazaadamantane cation in $[\text{2BH}]\text{BF}_4$ is protonated at a tertiary amine N atom. The resultant NH group donates three bifurcated hydrogen bonds, to the two geminal pyridyl groups and the BF_4^- ion (Fig. 7). The anion occupies a

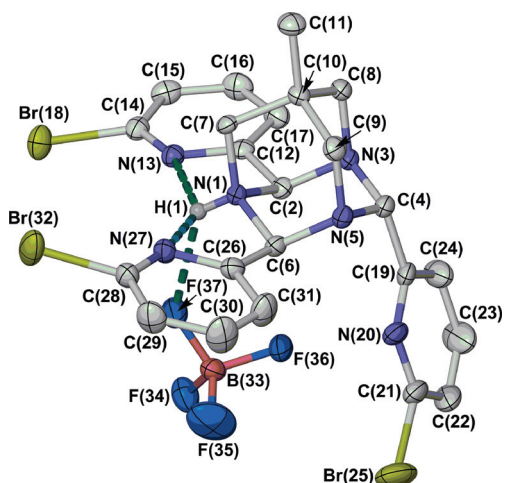


Fig. 7 View of the asymmetric unit in the crystal structure of $[2\text{BH}]^+$ BF_4^- . All H atoms have been omitted for clarity, and displacement ellipsoids are at the 50% probability level except for H(1) which has an arbitrary radius. Details of the additional intermolecular C–H...F interactions in the crystal are given in the ESI†. Colour code: C, white; H, grey; B, pink; Br, yellow; F, cyan; N, blue.

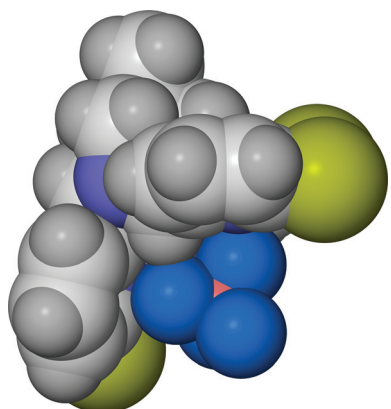
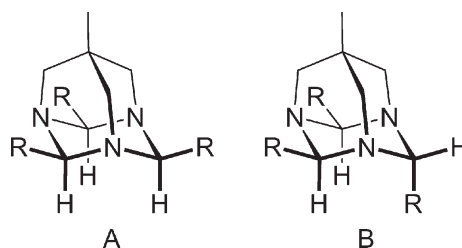


Fig. 8 Space-filling view of $[2\text{BH}]^+$ BF_4^- , showing the anion-binding pocket formed by the $[2\text{BH}]^+$ cation. All H atoms are included in the Figure. Other details as in Fig. 7.

pocket in the cation, formed by the triazahexane ring at the base of the $[2\text{BH}]^+$ cation and the face of the third, pendant pyridyl group (Fig. 8). In addition to the N–H...F hydrogen bond, shown in Fig. 7, there are several C–H...F interactions between the cation and the anion, the strongest of them involving two of the three aminal groups in the cation ($\text{H} \cdots \text{F} = 2.2$ – 2.3 Å, *ca.* 0.3 Å shorter than the sum of their van der Waals radii;³¹ ESI†). These interactions lead to a three-dimensional $(4^6 6^5)_2$ hydrogen bond network in the crystal, in which the cations and anions are both five-connected.

Notably, the 2,4,6-trypyridyl-1,3,5-triazaadamantane moieties in these structures adopt different geometric isomers. In $[\text{FeCl}_2(\mathbf{2C})]$, the three pyridyl groups all adopt equatorial positions with respect to the basal triazacyclohexyl ring (structure A, Scheme 2), while $\mathbf{2BH}^+$ contains two equatorial pyridyl substituents and one axial (structure B). The existence of these geometric isomers has been proposed previously, to account for the



Scheme 2 The two isomers of the 2,4,6-trisubstituted-7-methyl-1,3,5-triazaadamantane moiety observed in this work (R = pyridyl).

existence of multiple species in the ^1H NMR spectra of this class of compound.¹³ The ^1H NMR of $[\text{FeCl}_2(\mathbf{2C})]$ in $(\text{CD}_3)_2\text{CO}$ clearly shows the presence of two paramagnetic species in an 85 : 15 intensity ratio. These presumably correspond to isomers A and B in Scheme 2, with the uncoordinated pyridyl group occupying equatorial or basal coordination sites. Migration of the iron centre between the $\mathbf{2C}$ pyridyl groups does not occur on the NMR timescale, since distinct resonances for the free and coordinated pyridyl groups were clearly distinguished. However, the poor solubility of the complex in suitable solvents precluded high temperature NMR experiments, to determine whether isomers A and B interconvert in solution. The ^1H NMR spectrum of $[2\text{BH}]^+$ BF_4^- is strongly broadened, reflecting migration of the NH proton between the tertiary amine groups in the molecule.

Conclusions

In contrast to the $[\text{Fe}(\text{Py}_3\text{tren})]^{2+}$ podand system,^{17–23} replacement of the pyridyl donors in $[\text{Fe}(\text{Py}_3\text{tame})]^{2+}$ with more hindered or less basic heterocyclic donors does not lead to spin-crossover materials. This presumably reflects the conformational rigidity of the 2,2,2-*tris*(aminomethyl)ethane bridgehead unit of the Py₃tame podand, which may not be able to accommodate the expansion of the coordination sphere associated with a low→high spin transition. Notably, all the podand complexes in this work are also fully, or predominantly, low-spin in solution at room temperature by NMR. This contrasts with another complex in this series, bearing imidazol-4-yl substituents (an isomer of $[\text{Fe}(\mathbf{1E})]^{2+}$), which was reported to be high-spin in solution from UV-vis evidence.²⁵

This system is also complicated by the isomerisation of the podand ligands to 2,4,6-trisubstituted-7-methyl-1,3,5-triazaadamantanes, which are thermodynamically favoured in the absence of a strongly binding metal template and can themselves act as tridentate ligands. Monodentate coordination of unsubstituted 1,3,5-triazaadamantanes to d¹⁰ metal ions has been demonstrated previously,³² but these results show that these trisubstituted derivatives (which are facile to prepare) may have use as ligands for a variety of cations or anions. Molecular models imply that ligands of type 2 afford some steric control over the complexes they form, which could aid their use in coordination chemistry. In particular, six-coordinate complexes of type $[\text{M}(\mathbf{2})_2]^{2+}$ should be disfavoured, owing to steric repulsions between the heterocyclic groups of one ligand and the adamantyl core of the other (ESI†). Moreover, the C–H...X (X = Cl or F) hydrogen bonding

in $[\text{FeCl}_2(\mathbf{2C})]$ and $[\mathbf{2BH}]\text{BF}_4$ is of particular interest, since it suggests that 2,4,6-triaryl-1,3,5-triazaadamantanes may have value as anion binding sites in supramolecular chemistry or crystal engineering. We are currently investigating these possibilities.

Experimental

All reagents and solvents were used as commercially supplied, without further purification. Reactions were performed under an aerobic atmosphere. **CAUTION** Although we have experienced no problems with the perchlorate salt products in this work, metal–organic perchlorates are potentially explosive and should be handled with due care in small quantities.

Synthesis of $[\text{FeCl}_2(\mathbf{2C})] \cdot n\text{H}_2\text{O}$ ($n \approx 3/2$)

A mixture of 2-(aminomethyl)-2-methyl-1,3-diaminopropane *tris*-hydrochloride (0.25 g, 1.10 mmol) and NaOH (0.13 g, 3.30 mmol) in MeOH (50 cm³) was refluxed until all the solid had dissolved (*ca.* 30 mins). 6-Methylpyridine-2-carbaldehyde (0.40 g, 3.30 mmol) was then added to the solution, which was then refluxed for a further 30 min. Addition of $\text{Fe}[\text{BF}_4]_2 \cdot 6\text{H}_2\text{O}$ (0.37 g, 1.10 mmol) to the cooled, colourless solution caused the rapid development of a dark purple colouration. The solution was filtered, concentrated until the onset of precipitation, then stored at –30 °C overnight. The resultant lemon yellow solid was collected, washed with cold MeOH and Et₂O, and dried *in vacuo*. The product is sparingly soluble, but small amounts can be recrystallised from acetone–Et₂O. Yield 0.40 g, 63%. Found C, 53.6; H, 5.5; N, 14.4%. Calcd for $C_{26}\text{H}_{30}\text{Cl}_2\text{FeN}_6 \cdot 3/2\text{H}_2\text{O}$ C, 53.8; H, 5.7; N 14.5%. ESMS *m/z* 427 (100%, $[\mathbf{2CH}]^+$). IR (nujol) 3567 m, 3420 m, 2727 w, 1623 m, 1604 s, 1590 m, 1574 s, 1343 m, 1313 w, 1273 w, 1253 w, 1225 m, 1167 w, 1148 m, 1081 s, 1057 m, 1024 m, 1002 s, 986 s, 934 s, 909 w, 865 m, 850 m, 823 w, 794 s, 758 m, 738 w, 713 w, 662 w, 646 m, 637 s cm^{–1}. ¹H NMR ($\{\text{CD}_3\}_2\text{CO}$) δ –1.5 (br s, 1H, NCHN), –0.8 (br s, 2H, NCHN), 1.13 (s, 3H, CCH₃), 2.65 (s, 3H, uncoordinated PyCH₃), 3.3 (s, 2H, coordinated Py H⁴), 7.53 (d, 8.3 Hz, uncoordinated py H⁵), 7.77 (d, 8.6 Hz, uncoordinated py H³), Hz, 7.90 (pseudo-t, 7.9 Hz, 1H, uncoordinated Py H⁴), 12.5 and 12.9 (br s, both 2H, diastereotopic uncoordinated NCH₂C), 13.4 (v br s, 6H, coordinated PyCH₃), 25.5 (v br s, 2H, coordinated, NCH₂C), 49.7, 52.9 (both br s, 2H, coordinated Py H³ & H⁵). Some resonances from a second, minor isomer of the complex were also distinguishable, at 6.5, 6.6, 6.8, 10.0, 11.5, 49.0 and 52.5 ppm. The major : minor isomer integral ratio was 85 : 15.

Synthesis of $[\mathbf{2BH}]\text{BF}_4$

Method as above, using 6-bromopyridine-2-carbaldehyde (0.61 g, 3.30 mmol) yielded a yellow solution containing an off-white precipitate. The solid was collected by filtration, and recrystallised from MeNO₂–Et₂O. Yield 0.15 g, 19%. Found C, 39.2; H, 3.15; N, 11.7%. Calcd for $C_{23}\text{H}_{22}\text{BrF}_4\text{N}_6$ C 39.0; H 3.13; N 11.9%. ESMS *m/z* 620.9 (100%, $[\mathbf{2BH}]^+$). IR (nujol) 3362 br m, 3195 s, 3118 w, 3087 w, 2727 w, 1579 s, 1556 s, 1440 w, 1403 m, 1352 w, 1319 w, 1309 w, 1271 m, 1245 w,

1217 m, 1183 m, 1163 s, 1060 vs, 1001 m, 987 m, 941 w, 932 m, 923 w, 904 w, 871 m, 850 w, 831 m, 794 s, 784 s, 760 w, 736 m, 709 w, 678 s, 660 w, 645 m, 629 w, 619 m, 577 w cm^{–1}. ¹H NMR (CD₃NO₂) δ 0.72 (s, 3H, CCH₃), 3.32 and 3.66 (both br s, total integral 6H, CCH₂N), 5.71, 6.33 and 6.53 (all br s, total integral 3H, NCHN), 7.74 (br s, 3H, Py H⁵), 7.91 (br pseudo-t, 7.9 Hz, 3H, Py H⁴), 7.98 (d, 7.9 Hz, 3H, Py H³).

Synthesis of $[\text{Fe}(\mathbf{1C})]\text{[BF}_4\text{]}_2 \cdot 3\text{H}_2\text{O}$

A mixture of 2-(aminomethyl)-2-methyl-1,3-diaminopropane *tris*-hydrochloride (0.25 g, 1.10 mmol), NaOH (0.13 g, 3.30 mmol) and AgBF₄ (0.64 g, 3.30 mmol) were refluxed in EtOH (50 cm³) for 1 h. The solution was filtered, and Fe [BF₄]₂·6H₂O (0.37 g, 1.10 mmol) added. After 5 min stirring, 6-methylpyridine-2-carbaldehyde (0.40 g, 3.30 mmol) was added to the cloudy yellow–brown solution, which was then stirred at room temperature for 16 h. This yielded a purple solution, together with an off-white precipitate which was removed by filtration. Crystallisation of the concentrated filtrate with diethyl ether yielded a blue oil, together with a small number of pale green crystals which were removed by decantation. Recrystallisation of the oil from MeNO₂–Et₂O again yields an oily product, which could be solidified to a purple powder upon trituration with additional Et₂O. Yield 0.32 g, 41%. Found C, 44.0; H, 5.05; N, 11.7%. Calcd for $C_{26}\text{H}_{30}\text{B}_2\text{F}_8\text{FeN}_6 \cdot 3\text{H}_2\text{O}$ C, 44.0; H, 5.11; N, 11.8%. ESMS *m/z* 324 ($[\text{CH}_3\text{C}\{\text{CH}_2\text{NCHC}_5\text{H}_3\text{NCH}_3\}_2\text{CH}_2\text{NH}_2 + \text{H}]^+$), 427 ($[\text{LH}]^+$). ¹H NMR (CD₃NO₂) 1.56 (s, 3H, CCH₃), 1.78 (s, 9H, PyCH₃), 4.38 and 5.32 (both br m, 3H, CH₂), 7.98 (t, 7.8 Hz, 3H, Py H⁴), 9.57 and 9.92 (both d, 3H, Py H³ & H⁵), 14.90 (br s, 3H, NCH). The off-white impurity is probably **2C** or a salt of it, on the basis of its mass spectrum (*m/z* = 427.3 (100%, $[\mathbf{2CH}]^+$)). The ClO₄[–] salt of $[\text{Fe}(\mathbf{1C})]^{2+}$ has been reported previously, and does not have the same problems of solvent retention.²⁵

Synthesis of $[\text{Fe}(\mathbf{1D})]\text{[BF}_4\text{]}_2$

Method as above, using thiazole-2-carbaldehyde (0.37 g, 3.30 mmol). Concentration of the ethanol reaction mixture to *ca.* one-third its original volume was necessary to precipitate the product as a dark purple solid. The product was recrystallised from MeNO₂–Et₂O. Yield 0.32 g, 46%. Found C, 32.2; H, 2.90; N, 13.3%. Calcd for $C_{17}\text{H}_{18}\text{B}_2\text{F}_8\text{FeN}_6\text{S}_3$ C, 32.3; H, 2.87; N, 13.3%. ESMS *m/z* 229.0 (100%, $[\text{Fe}(\mathbf{1D})]^{2+}$). IR (nujol) 3133 w, 3112 m, 2725 w, 1572 m, 1557 s, 1486 m, 1405 m, 1367 w, 1350 m, 1316 m, 1308 w, 1284 m, 1213 s, 1181 s, 1148 w, 1060 vs, 933 w, 892 s, 797 m, 787 s, 765 s, 658 w, 621 m, 634 w, 567 w cm^{–1}. ¹H NMR (CD₃NO₂) δ 1.40 (s, 3H, CCH₃), 4.11 (br m, 6H, CH₂), 7.26 (d, 3.3 Hz, 3H, Tz H³), 8.30 (d, 3.3 Hz, 3H, Tz H⁴), 9.07 (s, 3H, NCH).

Synthesis of $[\text{Fe}(\mathbf{1E})]\text{[ClO}_4\text{]}_2$

Following the method for $[\text{Fe}(\mathbf{1C})]\text{[BF}_4\text{]}_2$, using imidazol-2-carbaldehyde, afforded a highly soluble wine red powder which was hard to recrystallise and did not give a good microanalysis. The perchlorate salt of the complex proved more tractable, and

Table 1 Experimental details for the single crystal structure determinations in this study

	[Fe(1E) ₂][ClO ₄] ₂ ·0.7H ₂ O	[Fe(1F) ₂][BF ₄] ₂	[Fe(1G) ₂][ClO ₄] ₂	[2BH]BF ₄	[FeCl ₂ (2C)] _n H ₂ O
Molecular formula	C ₁₇ H ₂₂ Cl ₂ FeN ₉ O _{8.7}	C ₂₀ H ₂₇ B ₂ F ₈ FeN ₉	C ₁₇ H ₂₁ Cl ₂ FeN ₉ O ₈	C ₂₃ H ₂₂ Br ₃ F ₄ N ₆	C ₂₆ H ₃₂ Cl ₂ FeN ₆ O
M _r	618.79	622.98	606.18	709.01	571.33
Crystal class	Triclinic	Monoclinic	Monoclinic	Monoclinic	Monoclinic
Space group	P $\bar{1}$	P 2_1	P $2_1/c$	P $2_1/c$	P $2_1/n$
a/ \AA	10.1387(13)	9.6735(16)	10.6707(14)	13.3839(10)	14.3647(12)
b/ \AA	12.1897(13)	15.700(2)	18.468(2)	8.7025(7)	15.4763(11)
c/ \AA	21.549(3)	9.9511(16)	12.6490(16)	23.2274(16)	26.538(2)
α ($^\circ$)	76.037(5)	—	—	—	—
β ($^\circ$)	87.449(7)	118.180(7)	94.781(6)	92.921(3)	103.818(5)
γ ($^\circ$)	75.601(4)	—	—	—	—
V/ \AA^3	2503.0(5)	1332.2(4)	2484.0(5)	2701.9(4)	5728.9(8)
Z	4	2	4	4	8
$\mu(\text{Mo-K}\alpha)/\text{mm}^{-1}$	0.881	0.651	0.884	4.531	0.740
T/K	150(2)	150(2)	150(2)	150(2)	150(2)
Measured reflections	91511	24349	102968	47518	212108
Independent reflections	14632	6288	7425	6637	13932
R _{int}	0.057	0.046	0.056	0.046	0.077
R(F) ^a	0.040	0.034	0.027	0.037	0.038
wR(F ²) ^b	0.107	0.069	0.072	0.089	0.103
Goodness of fit	1.042	1.001	1.047	1.013	1.035
Flack parameter	—	0.002(10)	—	—	—

$$^a R = \Sigma |F_o| - |F_c| / \Sigma |F_o|^2$$

$$^b wR = [\Sigma w(F_o^2 - F_c^2) / \Sigma wF_o^4]^{1/2}$$

was prepared as follows. A solution of 2-(aminomethyl)-2-methyl-1,3-diaminopropane *tris*-hydrochloride (0.25 g, 1.10 mmol) and NaOH (0.13 g, 3.30 mmol) in water (10 cm³), was added to another aqueous solution (25 cm³) of Fe[ClO₄]₂·6H₂O (0.40 g, 1.10 mmol) and imidazole-2-carbaldehyde (0.31 g, 3.30 mmol). The resultant blue-green mixture was stirred at 60 °C for 1 h, forming a dark red solution with some brown precipitate. The cooled solution was filtered and allowed to slowly evaporate under ambient conditions, yielding deep red crystals which gave an anhydrous powder when dried *in vacuo*. Yield 0.26 g, 39%. Found C, 34.2; H, 3.60; N, 21.3%. Calcd for C₁₇H₂₁Cl₂FeN₉O₈: C, 33.7; H, 3.49; N, 20.8%. ESMS *m/z* 203.6 (100%, [Fe(**1E**)²⁺]), 406.1 (18%, [⁵⁶Fe(**1E** – H)]⁺). IR (nujol) 3326 m, 3206 m, 3151 w, 3132 w, 2727 w, 1619 m, 1562 s, 1463 m, 1365 w, 1344 w, 1313 m, 1250 m, 1206 w, 1189 w, 1145 m, 1060 vs, 932 m, 923 w, 891 m, 881 m, 838 w, 798 w, 762 m, 709 w, 683 w, 621 m, 578 w cm⁻¹. ¹H NMR (CD₃NO₂) δ 1.30 (s, 3H, CCH₃), 4.03 (s, 6H, CH₂), 5.97 (br s, 3H, NH), 6.82 (br s, 3H, Im H⁵), 7.62 (br s, 3H, Im H⁴), 8.86 (s, 3H, NCH).

Synthesis of [Fe(**1F**)][BF₄]₂·H₂O

Method for [Fe(**1C**)][BF₄]₂, using 1-methyl-imidazole-2-carbaldehyde (0.36 g, 3.30 mmol). The product is a wine-red solid, that can be recrystallised from MeNO₂–Et₂O. Although the freshly crystallised complex does not contain lattice water by X-ray crystallography, IR and microanalytical data imply the bulk material is a hydrate phase. Yield 0.40 g, 58%. Found C, 37.2; H, 4.30; N, 19.4%. Calcd for C₂₀H₂₇B₂F₈FeN₉·H₂O C, 37.5; H, 4.56; N, 19.7%. ESMS *m/z* 197.6 (6%, [1FH]²⁺), 224.6 (100%, [Fe(**1F**)²⁺]), 394.2 (14%, [1FH]⁺), 536.2 (4%, [Fe(**1F**)(BF₄)]⁺). IR (nujol) 3585 m, 3123 m, 2726 w, 1650sh, 1634 m, 1570 s, 1538 w, 1425 m, 1344 w, 1321 w, 1290 s, 1216 w, 1206 m, 1180 m, 1050 vs, 934 m, 895 s, 840 w, 789 s, 778 s, 689 w, 665 m, 653 w, 625 m, 585 w cm⁻¹. ¹H NMR (CD₃NO₂) δ 1.32

(s, 3H, CCH₃), 3.99 (br m, 6H, CH₂), 4.08 (s, 9H, NCH₃), 6.72 (br s, 3H, Im H⁵), 7.46 (br s, 3H, Im H⁴), 8.86 (s, 3H, NCH).

Synthesis of [Fe(**1G**)][ClO₄]₂

The method for [Fe(**1C**)][BF₄]₂, using pyrazole-3-carbaldehyde, afforded an orange-red powder. This contained [Fe(**1G**)²⁺] by ESMS, but did not give a consistent microanalysis even after multiple recrystallisations. The perchlorate salt of this complex was prepared by the method described for [Fe(**1E**)][ClO₄]₂, using pyrazole-3-carbaldehyde (0.31 g, 3.30 mmol). Slow evaporation of the resultant red aqueous solution afforded brown crystals of the complex. Recrystallisation from MeNO₂–Et₂O was required to give an analytically pure product. Yield 0.16 g, 24%. Found C, 33.5; H, 3.45; N, 20.6%. Calcd for C₁₇H₂₁Cl₂FeN₉O₈: C, 33.7; H, 3.49; N, 20.8%. ESMS *m/z* 204.1 (64%, [⁵⁶Fe(**1G**)²⁺]), 407.1 (100%, [⁵⁶Fe(**1G** – H)]⁺), 506.1 (94%, [Fe(**1G**)(ClO₄)]⁺), 811.2 (68%, [Fe₂(**1G**)(**1G** – 3H)]⁺). ¹H NMR (CD₃NO₂): 1.34 (s, 3H, CCH₃), 4.56 (br m, 6H, CH₂), 7.31 (br s, 3H, Pz H⁴), 8.40 (br s, 3H, Pz H⁵), 10.20 (br s, 3H, Py NH), 11.68 (br s, 3H, NCH).

Single crystal X-ray structure determinations

Single crystals of [Fe(**1E**)][ClO₄]₂·0.7H₂O were grown by slow evaporation of an aqueous solution of the complex. Crystals of [Fe(**1F**)][BF₄]₂, [Fe(**1G**)][ClO₄]₂ and [**2BH**]BF₄ were obtained by slow diffusion of diethyl ether vapour into nitromethane solutions of the compounds, while [FeCl₂(**2C**)_nH₂O was similarly crystallised from acetone–diethyl ether. All diffraction data were measured using a Bruker X8 Apex diffractometer fitted with an Oxford Cryostream low temperature device, using graphite-monochromated Mo-K α radiation ($\lambda = 0.71073 \text{ \AA}$) generated by a rotating anode. Experimental details of the structure determinations in this study are given in Table 1. All the structures were

solved by direct methods (*SHELXS97*³³), and developed by full least-squares refinement on F^2 (*SHELXL97*³³). Crystallographic figures were prepared using *XSEED*,³⁴ which incorporates *POVRAY*.³⁵ Additional Figures of these crystal structures, and Tables of metric parameters, are given in the ESI†.

Single crystal X-ray structure of $[\text{Fe}(\text{1E})_2][\text{ClO}_4]_2 \cdot 0.7\text{H}_2\text{O}$

The asymmetric unit contains two complex cations, four perchlorate anions, one wholly occupied water molecule and one 40% occupied water site. The whole of cation Fe(1)–N(27), and the anions Cl(65)–O(69) and Cl(70)–O(74), are disordered over two sites, labelled ‘A’ (refined occupancy 0.60) and ‘B’ (refined occupancy 0.40). This disorder is coupled to the absence (orientation A) or presence (orientation B) of the partial water molecule O(76B), which lies close to N(27) and O(71). While the disorder models were constructed using bond length and angle restraints, these were removed for the final least squares cycles with no effect on the quality of the model. All non-H atoms were refined anisotropically, and C- and N-bound H atoms were placed in calculated positions and refined using a riding model. The H atoms on the wholly occupied water molecule O(75) were located in the Fourier map and allowed to refine subject to the fixed restraints O–H = 0.85(2) and H···H = 1.39(2) Å, with a displacement parameter equivalent to $1.2 \times$ that of the parent O atom. H atoms on the partial water site O(76B) were not located, but are included in the M_r and density calculations.

Single crystal X-ray structures of $[\text{Fe}(\text{1F})_2][\text{BF}_4]_2$, $[\text{Fe}(\text{1G})_2][\text{ClO}_4]_2$ and $[\text{2BH}] \text{BF}_4$

The structure of $[\text{Fe}(\text{1G})_2][\text{ClO}_4]_2$ was originally solved in the triclinic space group $P\bar{1}$, then transformed up to $P2_1/c$ using the *ADSYMM* routine in *PLATON*.³⁶ The other two of these structures refined successfully in the space groups they had originally been assigned (Table 1). No disorder was detected during refinement of any of these structures, and no restraints were applied to them. All non-H atoms were refined anisotropically, and all H atoms were placed in calculated positions and refined using a riding model.

Single crystal X-ray structure of $[\text{FeCl}_2(\text{2C})] \cdot n\text{H}_2\text{O}$ ($n \approx 1$)

The asymmetric unit contains two complex molecules, labelled ‘A’ and ‘B’, one crystallographically ordered water molecule, and a disordered region of solvent lying within channels in the lattice that was modelled using six partial water sites whose occupancies sum to 1. No disorder was present in the complex molecules, and no restraints were applied during refinement. All crystallographically ordered non-H atoms were refined anisotropically, while C-bound H atoms were placed in calculated positions and refined using a riding model. H atoms bound to the ordered water molecule were located in the Fourier map and allowed to refine freely. Hydrogen atoms from the disordered water sites were not included in the final model, but are included in the density calculation.

Other measurements

Electrospray (ES) mass spectra were performed with a Waters ZQ4000 TOF spectrometer using a MeCN feed solution. All peaks show correct isotopic distributions for their assigned molecular ions. CHN microanalyses were performed by the University of Leeds School of Chemistry microanalytical service. ^1H NMR spectra were run on a Bruker ARX300 spectrometer, operating at 300.1 MHz. IR spectra were run using a Nicolet Paragon 1000 spectrometer, using nujol mull samples held between NaCl windows. Room-temperature magnetic moments were measured using a Sherwood Scientific magnetic susceptibility balance. Molecular models were constructed using *CHEM3D*.³⁷

Acknowledgements

SAD is grateful to the University of St Thomas, St Paul, MN, USA and the University of Leeds for an exchange studentship. This work was funded by the above organisations, and by the EPSRC.

Notes and references

- 1 A. H. Ewald, R. L. Martin, I. G. Ross and A. H. White, *Proc. R. Soc. London, Ser. A*, 1964, **280**, 235.
- 2 *Spin Crossover in Transition Metal Compounds I-III, Top. Curr. Chem.*, ed. P. Gütlich and H. A. Goodwin, Springer-Verlag, Berlin, 2004, 233–235.
- 3 For recent reviews see: O. Sato, J. Tao and Y.-Z. Zhang, *Angew. Chem., Int. Ed.*, 2007, **46**, 2152; P. Gamez, J. S. Costa, M. Quesada and G. Aromí, *Dalton Trans.*, 2009, 7845; M. A. Halcrow, *Chem. Soc. Rev.*, 2011, **40**, 4119.
- 4 O. Kahn and C. J. Martinez, *Science*, 1998, **279**, 44.
- 5 R. N. Muller, L. Vander Elst and S. Laurent, *J. Am. Chem. Soc.*, 2003, **125**, 8405.
- 6 J. Krober, E. Codjovi, O. Kahn, F. Grolière and C. Jay, *J. Am. Chem. Soc.*, 1993, **115**, 9810; C. Rajadurai, O. Fuhr, R. Kruk, M. Ghafari, H. Hahn and M. Ruben, *Chem. Commun.*, 2007, 2636.
- 7 Y. Bodenthin, G. Schwarz, Z. Tomkowicz, M. Lommel, T. Geue, W. Haase, H. Möhwald, U. Pietsch and D. G. Kurth, *Coord. Chem. Rev.*, 2009, **293**, 2414.
- 8 A. B. Gaspar, M. Seredyuk and P. Gütlich, *Coord. Chem. Rev.*, 2009, **293**, 2399.
- 9 A. Bousseksou, G. Molnár, L. Salmon and W. Nicolazzi, *Chem. Soc. Rev.*, 2011, **40**, 3313 and references therein
- 10 G. Aromí, L. A. Barrios, O. Roubeau and P. Gamez, *Coord. Chem. Rev.*, 2011, **255**, 485.
- 11 M. C. Muñoz and J. A. Real, *Coord. Chem. Rev.*, 2011, **255**, 2068.
- 12 I. Šalitroš, N. T. Madhu, R. Boča, J. Pavlik and M. Ruben, *Monatsh. Chem.*, 2009, **140**, 695.
- 13 D. A. Durham, F. A. Hart and D. Shaw, *J. Inorg. Nucl. Chem.*, 1967, **29**, 509.
- 14 E. B. Fleischer, A. E. Gebala and P. A. Tasker, *J. Am. Chem. Soc.*, 1970, **92**, 6365; S. O. Wandiga, J. E. Sarneski and F. L. Urbach, *Inorg. Chem.*, 1972, **11**, 1349; E. Larsen, G. K. La Mar, B. E. Wagner, J. E. Parks and R. H. Holm, *Inorg. Chem.*, 1972, **11**, 2652; E. B. Fleischer, A. E. Gebala, D. R. Swift and P. A. Tasker, *Inorg. Chem.*, 1972, **11**, 2775; W. M. Reiff, *J. Am. Chem. Soc.*, 1973, **95**, 3048.
- 15 F. L. Urbach and S. O. Wandiga, *J. Chem. Soc. D*, 1970, 1572.
- 16 M. Seredyuk, A. B. Gaspar, V. Ksenofontov, Y. Galyametdinov, J. Kusz and P. Gütlich, *Adv. Funct. Mater.*, 2008, **18**, 2089.
- 17 M. A. Hoselton, L. J. Wilson and R. S. Drago, *J. Am. Chem. Soc.*, 1975, **97**, 1722; L. J. Wilson, D. Georges and M. A. Hoselton, *Inorg. Chem.*, 1975, **14**, 2968; M. S. Lazarus, M. A. Hoselton and T. S. Chou, *Inorg. Chem.*, 1977, **16**, 2549; W. H. Batschelet and N. J. Rose, *Inorg. Chem.*, 1983, **22**, 2083; A. J. Conti, C.-L. Xie and D. N. Hendrickson, *J. Am. Chem. Soc.*, 1989, **111**, 1171; M. Seredyuk, A. B. Gaspar, J. Kusz, G. Bednarek and P. Gütlich, *J. Appl. Crystallogr.*, 2007, **40**, 1135.

- 18 C. Brewer, G. Brewer, C. Luckett, G. S. Marbury, C. Viragh, A. M. Beatty and W. R. Scheidt, *Inorg. Chem.*, 2004, **43**, 2402; C. Brewer, G. Brewer, G. Patil, Y. Sun, C. Viragh and R. J. Butcher, *Inorg. Chim. Acta*, 2005, **358**, 3441; G. Brewer, R. J. Butcher, C. Viragh and G. White, *Dalton Trans.*, 2007, 4132; L. Alvarado, C. Brewer, G. Brewer, R. J. Butcher, A. Straka and C. Viragh, *CrystEngComm*, 2009, **11**, 2297.
- 19 C. Brewer, G. Brewer, C. Luckett and G. S. Marbury, *Inorg. Chem.*, 2004, **43**, 2402; H. Ohta, Y. Sunatsuki, M. Kojima, S. Iijima, H. Akashi and N. Matsumoto, *Chem. Lett.*, 2004, **33**, 350; M. Yamada, E. Fukumoto, M. Ooidemizu, N. Bréfuel, N. Matsumoto, S. Iijima, M. Kojima, N. Re, F. Dahan and J.-P. Tuchagues, *Inorg. Chem.*, 2005, **44**, 6967; M. Yamada, H. Hagiwara, H. Torigoe, N. Matsumoto, M. Kojima, F. Dahan, J.-P. Tuchagues, N. Re and S. Iijima, *Chem.-Eur. J.*, 2006, **12**, 4536.
- 20 Y. Ikuta, M. Ooidemizu, Y. Yamahata, M. Yamada, S. Osa, N. Matsumoto, S. Iijima, Y. Sunatsuki, M. Kojima, F. Dahan and J.-P. Tuchagues, *Inorg. Chem.*, 2003, **42**, 7001; Y. Sunatsuki, H. Ohta, M. Kojima, Y. Ikuta, Y. Goto, N. Matsumoto, S. Iijima, H. Akashi, S. Kaizaki, F. Dahan and J.-P. Tuchagues, *Inorg. Chem.*, 2004, **43**, 4154.
- 21 Y. Sunatsuki, Y. Ikuta, N. Matsumoto, H. Ohta, M. Kojima, S. Iijima, S. Hayami, Y. Maeda, S. Kaizaki, F. Dahan and J.-P. Tuchagues, *Angew. Chem., Int. Ed.*, 2003, **42**, 1614; M. Yamada, M. Ooidemizu, Y. Ikuta, S. Osa, N. Matsumoto, S. Iijima, M. Kojima, F. Dahan and J.-P. Tuchagues, *Inorg. Chem.*, 2003, **42**, 8406.
- 22 H. Z. Lazar, T. Forestier, S. A. Barrett, C. A. Kilner, J.-F. Létard and M. A. Halcrow, *Dalton Trans.*, 2007, 4276.
- 23 C. T. Brewer, G. Brewer, R. J. Butcher, E. E. Carpenter, A. M. Schmiedekamp and C. Viragh, *Dalton Trans.*, 2007, 295.
- 24 M. A. Halcrow, *Coord. Chem. Rev.*, 2009, **253**, 2493 and references therein
- 25 M. Seredyuk, A. B. Gaspar, J. Kusz and P. Gütlich, *Z. Anorg. Allg. Chem.*, 2011, **637**, 965.
- 26 E. König, *Prog. Inorg. Chem.*, 1987, **35**, 527.
- 27 B. Weber and F. A. Walker, *Inorg. Chem.*, 2007, **46**, 6794.
- 28 See e.g. J. Elhaïk, C. A. Kilner and M. A. Halcrow, *CrystEngComm*, 2005, **7**, 151; R. Pritchard, S. A. Barrett, C. A. Kilner and M. A. Halcrow, *Dalton Trans.*, 2008, 3159, and 2009, 10622 (correction); R. Pritchard, H. Lazar, S. A. Barrett, C. A. Kilner, S. Asthana, C. Carbonera, J.-F. Létard and M. A. Halcrow, *Dalton Trans.*, 2009, 6656.
- 29 R. K. O'Reilly, V. C. Gibson, A. J. P. White and D. J. Williams, *Polyhedron*, 2004, **23**, 2921.
- 30 A. W. Addison, T. N. Rao, J. Reedijk, J. van Rijn and G. C. Verschoor, *J. Chem. Soc., Dalton Trans.*, 1984, 1349. An ideal square pyramidal structure gives $\tau = 0$, while a perfect trigonal pyramidal geometry gives $\tau = 1$
- 31 L. Pauling, *The Nature of the Chemical Bond*, Cornell University Press, Ithaca, NY, USA, 3rd edn, 1960, pp. 257–264.
- 32 A. F. Danil de Namor, N. A. Nwogu, J. A. Zvietcovich-Guerra, O. E. Piro and E. E. Castellano, *J. Phys. Chem. B*, 2009, **113**, 4775.
- 33 G. M. Sheldrick, *Acta Crystallogr., Sect. A: Found. Crystallogr.*, 2008, **64**, 112.
- 34 L. J. Barbour, *J. Supramol. Chem.*, 2001, **1**, 189.
- 35 POVRAY v. 3.5, Persistence of Vision Raytracer Pty. Ltd., Williamstown, Victoria, Australia, 2002. <http://www.povray.org>
- 36 A. L. Spek, *J. Appl. Crystallogr.*, 2003, **36**, 7.
- 37 CHEM3D Ultra, v. 7.0, CambridgeSoft, Cambridge MA, USA, 2001